Climate Dynamics (2018) 51:2913–2925
https://doi.org/10.1007/s00382-017-4056-4

Regional climate of the Subtropical Central Andes using high-resolution CMIP5 models. Part II: future projections for the twenty-first century

Natalia Zazulie[1,2,3] · **Matilde Rusticucci**[1,2,3] · **Graciela B. Raga**[4]

Received: 18 May 2017 / Accepted: 14 December 2017 / Published online: 27 December 2017

Abstract
In Part I of our study (Zazulie et al. Clim Dyn, 2017, hereafter Z17) we analyzed the ability of a subset of fifteen high-resolution global climate models (GCMs) from the Coupled Model Intercomparison Project phase 5 to reproduce the past climate of the Subtropical Central Andes (SCA) of Argentina and Chile. A subset of only five GCMs was shown to reproduce well the past climate (1980–2005), for austral summer and winter. In this study we analyze future climate projections for the twenty-first century over this complex orography region using those five GCMs. We evaluate the projections under two of the representative concentration pathways considered as future scenarios: RCP4.5 and RCP8.5. Future projections indicate warming during the twenty-first century over the SCA region, especially pronounced over the mountains. Projections of warming at high elevations in the SCA depend on altitude, and are larger than the projected global mean warming. This phenomenon is expected to strengthen by the end of the century under the high-emission scenario. Increases in winter temperatures of up to 2.5 °C, relative to 1980–2005, are projected by 2040–2065, while a 5 °C warming is expected at the highest elevations by 2075–2100. Such a large monthly-mean warming during winter would most likely result in snowpack melting by late winter-early spring, with serious implication for water availability during summer, when precipitation is a minimum over the mountains. We also explore changes in the albedo, as a contributing factor affecting the net flux of energy at the surface and found a reduction in albedo of 20–60% at high elevations, related to the elevation dependent warming. Furthermore, a decrease in winter precipitation is projected in central Chile by the end of the century, independent of the scenario considered.

Keywords CMIP5 models · Model evaluation · Subtropical Central Andes · Future projections · Elevation-dependent warming

1 Introduction

Global warming since the late nineteenth century is evident over land and ocean, and the past three decades have been successively warmer at the Earth's surface than any of the previous decades in the instrumental record. Nevertheless, the surface warming is not spatially uniform (Stocker et al. 2013), with different regions experiencing different warming rates, the Arctic being the most notorious example. Mountainous regions appear to be more sensitive to global-scale warming than other regions at lower elevations but at the same latitude (Beniston et al. 1997; Bradley et al. 2004; Rangwala et al. 2013). Mountainous regions generally are home to fragile ecosystems, and glaciers and the seasonal snowpack constitute key sources of freshwater for the adjacent lowlands (Beniston 2003; Viviroli et al. 2007). There

✉ Natalia Zazulie
nzazulie@at.fcen.uba.ar

[1] Departamento de Ciencias de la Atmósfera y los Océanos, FCEN, Universidad de Buenos Aires, Buenos Aires, Argentina

[2] Consejo Nacional de Investigaciones Científicas y Técnicas (CONICET), Buenos Aires, Argentina

[3] Unidad Mixta Internacional – Instituto Franco-Argentino para el Estudio del Clima y sus Impactos (UMI-IFAECI), Facultad de Ciencias Exactas y Naturales, Universidad de Buenos Aires, Buenos Aires, Argentina

[4] Centro de Ciencias de la Atmósfera, Universidad Nacional Autónoma de Mexico, Mexico City, Mexico

is an ongoing and growing need for reliable and up-to-date climate change information at the local-to-regional scales in order to effectively manage future climate risk (Zubler et al. 2015). Due to the role that mountains play in terms of resources provided to both local and lowland communities, it is important to determine the future trends of climate in mountainous regions and whether these regions will experience stronger warming compared to adjacent lowlands and to the global mean (Palazzi et al. 2016).

Several studies have addressed future projections for mountainous regions around the world from Global Climate Model (GCM) simulations and have highlighted the issue of the elevation dependent warming (EDW)—the altitudinal dependence of warming rates—due to its implications for future rates of change in mountain cryosphere systems and their associated hydrological regimes, mountain ecosystems and biodiversity (Rangwala et al. 2016; Pepin et al. 2015; Bradley et al. 2006). Since temperature at the Earth's surface is primarily the result of the radiative energy balance, the factors that affect the net flux of radiation at the surface such as albedo, clouds, water vapor and related feedbacks (Palazzi et al. 2016), among others, are the potential drivers of the EDW. Pepin et al. (2015) present a review on the different mechanisms that contribute towards EDW. They point out that the resulting response to all these factors and their interactions is complex, and some of them will be more influential than others in different regions and at certain times of the year. As an example, Fyfe and Flato (1999) analyzed a single GCM simulation for the US Rocky Mountains and found enhanced warming at higher elevations during winter and spring due to a rise in the snow line, which amplifies the surface warming via the snow-albedo feedback. Liu et al. (2009) analyzed both observations and model projections for the Tibetan Plateau and found an amplified warming in monthly minimum temperatures at higher elevations, particularly in winter and spring, likely caused by a combination of cloud-radiation and snow-albedo feedbacks. Rangwala et al. (2013) analyzed future projection for the Himalayas in Asia and the Rocky Mountains in the United States and concluded that at higher elevations warming is enhanced relative to lowlands at the same latitudes, particularly in the cold season, with no significant summer warming. In a recent study, Palazzi et al. (2016) analyzed the EDW over the Tibetan Plateau using simulations from GCMs participating in the Coupled Model Intercomparison Project phase 5 (CMIP5). They found the largest warming in regions with mean temperatures below freezing especially in winter, suggesting a key role of mechanisms involving water phase changes, the presence/absence of snow and the snow-albedo feedback.

The tropical Andes in South America have been the focus of attention due to the rapid decrease of mountain glaciers related to global warming (Bradley et al. 2006; Vuille et al. 2008). Palomino-Lemus et al. (2015) studied summer projections over the Andes of Colombia applying statistical downscaling of CMIP5 GCMs and found that liquid precipitation will increase over this region in the period 2071–2100. In a recent study, Rangecroft et al. (2016) explored future projections for the Bolivian Andes and concluded that a dramatic loss of the extent of the permafrost is expected in response to projected twenty-first century warming, representing a reduction of high mountain water storage.

Recent precipitation trends for central Chile and central-western Argentina reported by different studies, indicate decreasing trends in annual precipitation in central Chile during the twentieth century, in contrast with the increase observed east of the Andes, over the lowlands of Argentina (Aceituno et al. 1993; Minetti and Vargas 1998; Barros et al. 2000; Minetti et al. 2003). Minetti et al. (2003) found a decreasing trend in annual precipitation between 1931 and 1999 in a broad region that included central Chile, high-altitude sections of the Cuyo Cordillera and Comahue in Argentina, which encompasses the SCA region. Rosenblüth et al. (1997) studied temperature trends in Argentina and Chile, over the period 1960–1992, and found an increase in annual and seasonal temperature in central Chile (from stations Punta Tortuga and Punta Angeles, Chile) and a cooling east of the Andes (from Mendoza station, Argentina). Falvey and Garreaud (2009) reported decreasing trends of annual temperature near the coast of Chile and warming inland over the period 1979–2006. Vincent et al. (2005) studied temperature extreme indices and found opposite behavior on either side of the Andes: warming on the west and cooling on the east over Argentina for the period 1961–2000. According to Barros et al. (2015), instrumental observations and paleoclimate proxy data over the Andes Mountains between 30° and 40°S indicate a positive trend in temperature, especially in winter, and a declining trend in annual precipitation. These trends have caused a reduction of the ice mass in the Andes and glacier retreats have been observed since the nineteenth century (Le Quesne et al. 2009). In particular, winter precipitation and temperature trends for the SCA of Argentina and Chile were studied by Rusticucci et al. (2014) over the period 1979–2010. The study, using different gridded datasets and ERA-Interim reanalysis, indicates a generalized decrease in winter precipitation and warming especially between 32° and 35°S.

Future twenty-first century projections for South America indicate a significant warming and decrease in precipitation for southern-central Chile and increased precipitation over the plains of southeastern South America (Blazquez and Nuñez 2013; Barros et al. 2015). Barros et al. (2015) highlight that the projected temperature increase over Argentina for the coming decades is greater than the observed warming of the last 60 years, and will occur over only 30 years. This constitutes an acceleration in the regional warming rate.

However, updated future projections using the most recent generation of GCMs for the subtropical Andes have not been carried out and there are no published studies on the EDW over this region.

The Andes mountain range acts as a topographic barrier to the atmospheric flow from the deep tropics to mid-latitudes; its highest peaks and ridges constitute the border between Argentina and Chile between 23° and 53°S. The Andes between 30° and 37°S are of particular importance since they separate two large agricultural and industrial regions: central Chile to the west and the lowlands of western Argentina to the east. The annual snowpack is a critical source of river runoff, contributing to the socio-economical activities of the nearby population (Masiokas et al. 2006; Barros et al. 2015). Water availability affects human consumption, irrigation, hydro-electric power generation and industries. This region is highly vulnerable to changes in climate, particularly to a warming scenario that will directly affect its cryosphere; therefore, it is crucial to provide regional information of future projections. The aim of this study is to analyze future climate projections for the complex orography region of the Subtropical Central Andes using high-resolution GCMs from CMIP5 for the twenty-first century. The present study also aims to analyze the dependence of projected changes on elevation in this region and to evaluate if the reduction of the cryosphere—through the analysis of surface albedo—could be one of the possible mechanisms leading to the EDW.

2 Data and methods

We analyze climate simulations of the twenty-first century performed by a selection of high-resolution models participating in CMIP5 (Taylor et al. 2012). We select two of the four representative concentration pathways (RCPs) designed as future scenarios for the CMIP5: RCP4.5 and RCP8.5. A detailed description of the different future scenarios can be found in Moss et al. (2010). The RCPs considered in this study correspond to an intermediate stabilization scenario and a high emission scenario, respectively (van Vuuren et al. 2011). Radiative forcing in RCP4.5 stabilizes at 4.5 W/m^2 (approximately 650 ppm CO_2-equivalent) in the year 2100 without ever exceeding that value (Thomson et al. 2011). In the RCP8.5 the greenhouse gas emissions and concentrations increase considerably over time, leading to a radiative forcing of 8.5 W/m^2 (~940 ppm CO_2) at the end of the century (Riahi et al. 2011). Model outputs were obtained from the data archives of the Program for Climate Model Diagnosis and Intercomparison (PCMDI, http://www-pcmdi.llnl.gov). We consider only one realization of each selected climate model and we analyze the following set of variables: surface altitude (orog), near surface temperature (tas), precipitation (pr), surface downwelling shortwave radiation (rsds), surface upwelling shortwave radiation (rsus), sea level pressure (psl), specific humidity (hus), eastward wind (ua) and northward wind (va). Surface albedo was calculated as the ratio between the surface upwelling and downwelling shortwave radiation.

In our previous study (Z17) we analyzed the ability of fifteen high-resolution CMIP5 GCMs (for full list see Table 1 in Z17) to reproduce the past climate of the Subtropical Central Andes, against two reference datasets: ERA-Interim reanalysis and CRU gridded dataset over the period 1980–2005 for austral summer and winter. The studied region is concentrated over the Andes between 30°–37°S and 71°–69.5°W and location and topography of the SCA box can be seen in Fig. 1 from Z17. The analysis presented in Z17 showed that a subset of GCMs performed better than the multi-model ensemble mean (MMM15) in the past: BCC-CCSM1(m), CCSM4, CESM1-CAM5, CNRM-CM5 and EC-EARTH. Therefore, a five-member ensemble (MMM5) was produced from these models to analyze future climate projections in the selected Andean region. While MIROC4h also performed well for 1980–2005, simulations were not available for the twenty-first century so this model was not included in the MMM15. Since only RCP8.5 simulations were available from the MRI-ESM1, this model is only present in the

Table 1 Temperature (°C/decade) and precipitation trends ((mm/day)/decade) for the period 2006–2100

	Temperature (°C/decade)				Precipitation, (mm/day)/decade			
	DJF		JJA		DJF		JJA	
	RCP4.5	RCP8.5	RCP4.5	RCP8.5	RCP4.5	RCP8.5	RCP4.5	RCP8.5
BCC-CSM1.1 (m)	**0.11**	**0.39**	**0.08**	**0.26**	0	0	−0.01	−0.01
CCSM4	**0.17**	**0.42**	**0.16**	**0.38**	0	**0.04**	−0.01	**−0.10**
CESM1 (CAM5)	**0.25**	**0.52**	**0.30**	**0.59**	0.01	0.01	0.06	0.06
CNRM-CM5	**0.28**	**0.53**	**0.22**	**0.53**	0	−0.01	0	−0.04
EC-EARTH	**0.22**	**0.49**	**0.23**	**0.55**	0	−0.01	−0.04	**−0.11**
MMM5	**0.21**	**0.47**	**0.20**	**0.46**	0	0	0	−0.04

Significant trends at the 95% level of confidence are shown in bold

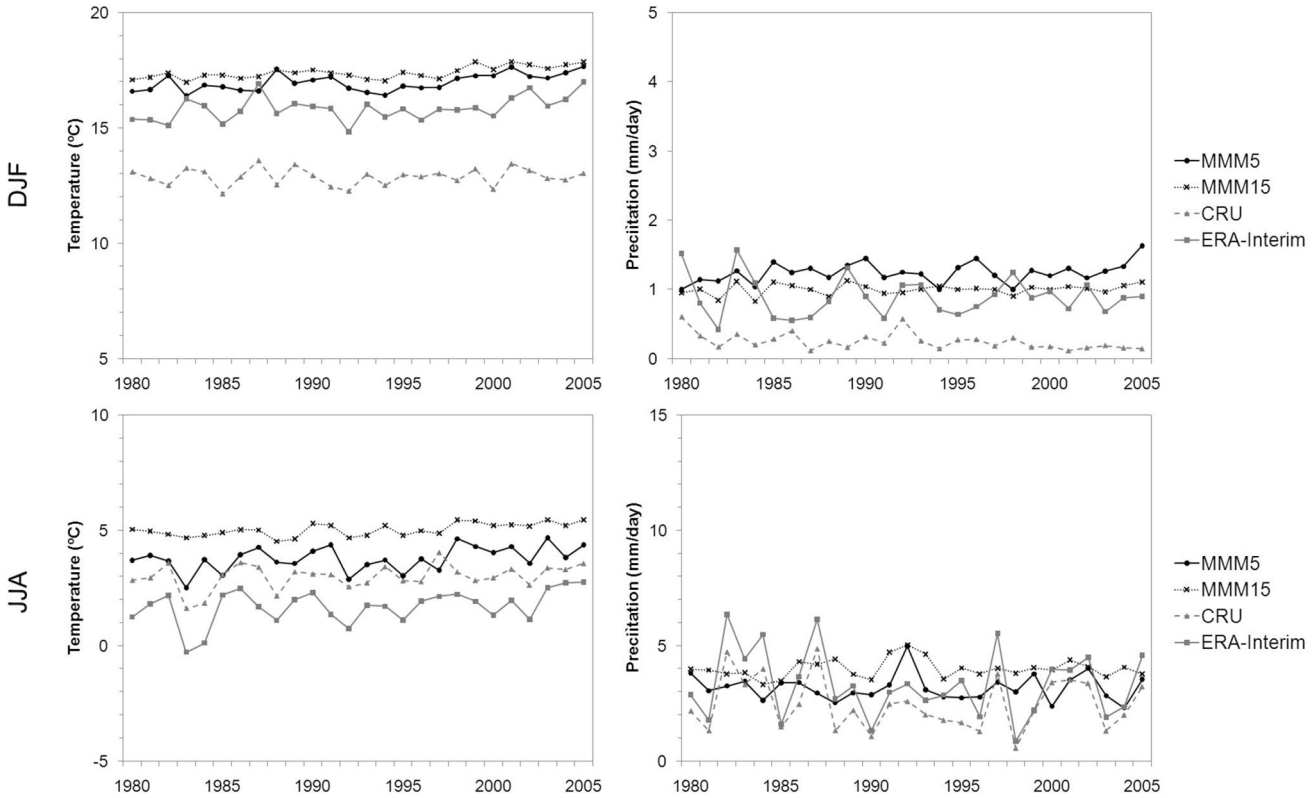

Fig. 1 Temporal series of areal mean of near surface temperature (left) and precipitation (right) over the SCA box for the period 1980–2005. In grey the reference datasets (dashed and triangles: CRU; line and squares: ERA-Interim) and in black the multi-model means (lines and circles: MMM5 with 5 GCMs; dotted and crosses: MMM15 with all GCMs)

MMM15 for that scenario. We compare here the results from the multi model ensemble mean from the original 15 GCMs evaluated in Z17, with the reduced, five-member ensemble.

As in Z17, the region of the Subtropical Central Andes (SCA) is delimited by 30°–37°S and 71°–69.5°W; austral summer season corresponds to December–January–February and austral winter season to June–July–August, respectively. Results are presented here in terms of temporal evolution of temperature and precipitation for the period 2006–2100, spatially averaged over the SCA box. We also analyze spatial patterns of change for two periods: 2040–2065 and 2075–2100 relative to the historical period 1980–2005 for each season.

3 Results

Figure 1 shows time series of temperature and precipitation averaged over the SCA box for the multi-model mean considering the fifteen GCMs (MMM15) initially proposed by Z17 and the reduced ensemble with the selected five GCMs (MMM5). This figure also shows the interannual variability of temperature and precipitation for the summer and winter seasons, as represented by the two reference datasets—CRU and ERA-Interim, shown in grey—for the period 1980–2005. ERA-Interim reanalysis has been validated over this region in Rusticucci et al. (2014) against different gridded datasets and meteorological stations for winter season (Viale and Nuñez 2011). A good representation of both interannual variability and trends was found in the period 1979–2010. In Fig. 1, note firstly that the reference datasets show better agreement between them in winter (JJA) than in summer (DJF). As was discussed in Z17, the CRU dataset better represents the temperature in the SCA region, with reanalysis showing a warm bias (almost 3 °C) in summer. Both ensembles (MMM15 and MMM5) overestimate summer temperature over the entire period. Nevertheless, the reduced ensemble MMM5 shows a slight improvement, as seen by lower values of summer temperature compared to those from the MMM15. During winter, the mean difference between the reference datasets is reduced to approximately 1 °C, and the improvement with the reduced ensemble is more noticeable. MMM5 shows not only a better agreement with the validation datasets in the mean value, but also in the interannual variability assessed in Z17 through the monthly coefficient of variation. As pointed out in Z17, GCMs overestimate interannual variability in every month. Furthermore, Z17 shows a generalized agreement in the long-term

behavior between GCMs and the reference datasets, with warming in both seasons.

As also discussed in Z17, there is a generalized misrepresentation by GCMS in the processes involved in summer convective precipitation east of the Andes, in Argentina. This results in an overestimate of summer precipitation both by GCMs and reanalysis in the eastern edge of the SCA box, which affects the areal average. There is a mean difference of 0.6 mm/day between the reanalysis and the CRU, which is quite large considering the observed mean value for the season (0.25 mm/day). The reduced ensemble MMM5 does not perform better than the MMM15 in this case. In contrast, both reference datasets agree in the winter precipitation mean and its interannual variability, indicative of a good representation of the mechanisms involved in winter precipitation by the reanalysis, as was discussed in another of our studies of climate in the region (Rusticucci et al. 2014). The reduced ensemble MMM5 outperforms the MMM15 in the mean values and interannual variability for winter precipitation, compared with the reference datasets. While both reference datasets coincide in the sign of the precipitation trends in each season, there is no agreement among GCMs in the long-term behavior of this variable, according to Z17.

The mean annual cycle of temperature for the MMM5, as expected, shows a systematic increase throughout the year for both RCPs, highest for RCP8.5 and end of the century time frame (Fig. 2). The mean annual cycle of precipitation is projected to shift slightly from a current winter maximum in June to a broader maximum for June–July by mid-century and a decrease in magnitude by the end of the century. As in the current climate, summer precipitation is much lower than winter precipitation in the SCA region; while there is an indication of higher summer precipitation, this should

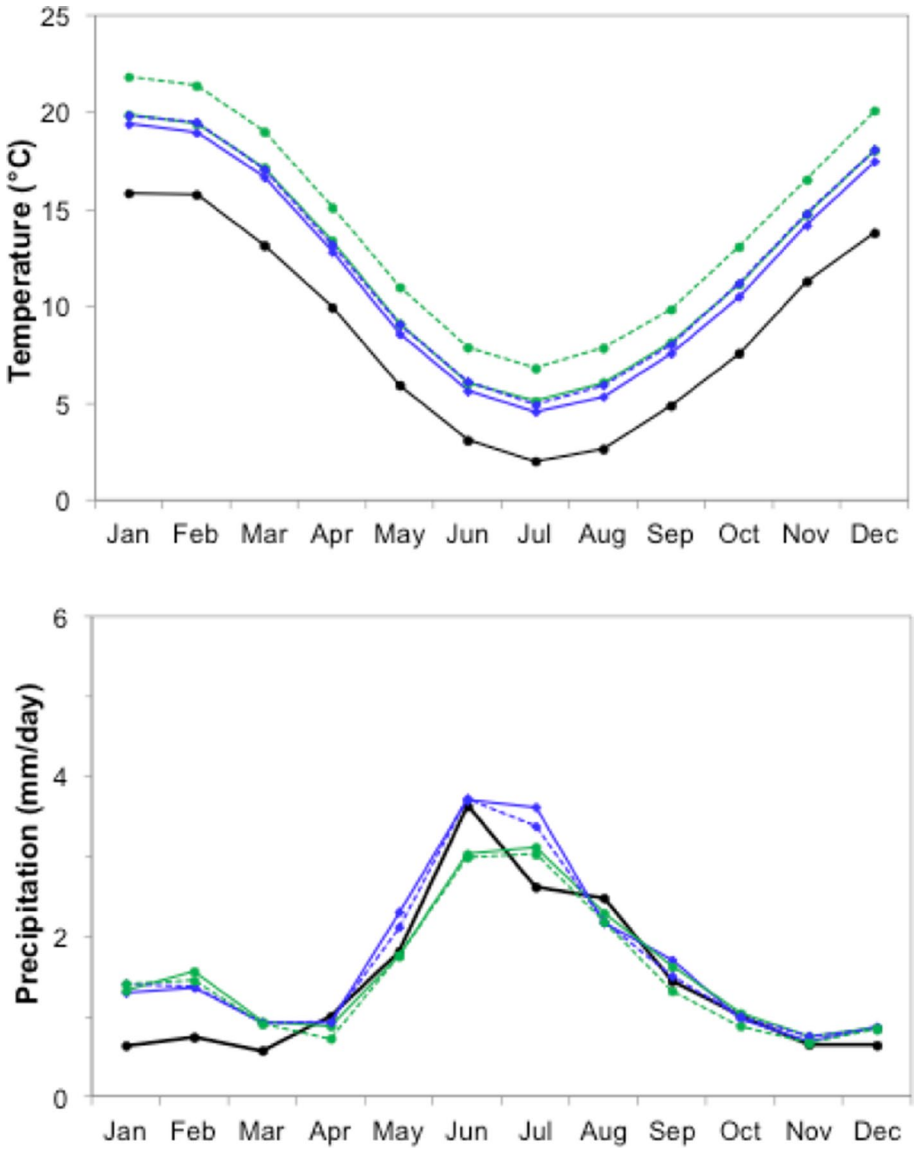

Fig. 2 Annual cycle of mean temperature (upper pannel) and mean precipitation (lower pannel) averaged over the SCA box for the historical period 1980–2005 (black lines), and simulated future: 2040-65, blue and 2075–2100, green. The two scenarios are plotted: solid lines: RCP4.5 and dashed lines: RCP8.5

be considered with caution given the errors in representing summer precipitation in the current climate.

The projected near surface temperature time series from 2006 to 2100, averaged over the SCA region for summer (DJF) and winter (JJA) for the two RCPs, are shown in Fig. 3. The black line shows the five-member ensemble (MMM5), the dotted line corresponds to the MMM15 and the shaded grey area indicates the spread among their respective members. Both scenarios show warming trends for summer and winter. The projected MMM15 is higher than the reduced ensemble for both scenarios and in both seasons, more evident in winter than in summer where the difference between ensembles is 1 °C. Naturally, the spread is reduced when a smaller number of members is included in the ensemble mean but this fact is more evident in winter. By the end of the twenty-first century, all cases show a reduced spread (shaded grey area). Table 1 shows the temperature trends for the twenty-first century derived from each of the five GCMs and the MMM5. A Student's t test was applied to assess the significance of the trends. Significant values at the 95% level of confidence indicated in bold in Table 1. Each of the GCMs, as well as the MMM5, shows significant positive trends, reinforcing the robustness of the signal in this region. As expected, the simulations for the RCP8.5 show a larger increase (0.47°/decade) than for the RCP4.5 (0.21°/decade) during summer. In winter, the two scenarios show similar increasing trends as in summer, in each GCM and the MMM5: 0.20°/decade for RCP4.5 and 0.46°/decade for RCP8.5.

The projected MMM5 and MMM15 precipitation in the SCA region for both seasons and scenarios are shown in Fig. 4, where the y-axis is adjusted to the climatological values for each season. The projections indicate that precipitation remains at around 1 mm/day in summer, with small interannual variability and small spread between members. Summer values are slightly higher for the MMM5 than for the MMM15. During winter, when most of the precipitation is observed over the Subtropical Central Andes region, projections indicate no significant changes for either of the scenarios. Values of MMM15 are higher than those of MMM5, and MMM15 (light grey shading) shows more variability than MMM5. None of the scenarios indicates significant changes.

All GCMs and MMM5 indicate virtually null trends in summer precipitation for RCP4.5 (Table 1). Only CCSM4 shows a significant positive trend for the RCP8.5, but there is not agreement among models. Most models show a negative trend in winter precipitation, with two GCMs showing

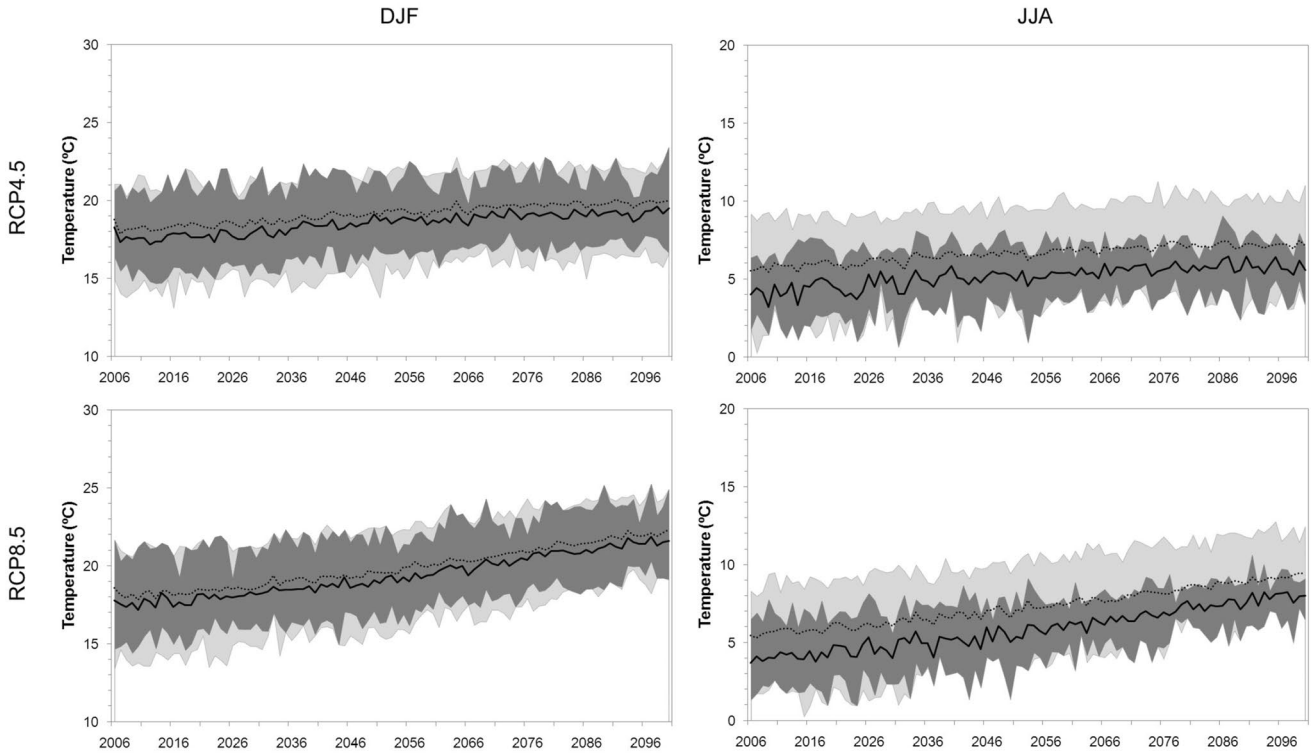

Fig. 3 Temporal series of projected near surface temperature spatially averaged over the SCA box for the period 2006–2100. Dotted lines correspond to MMM with all GCMs and solid line corresponds to the reduced ensemble with 5 GCMs. Shaded areas indicate the spread among GCMs (light grey: all GCMs; dark grey: reduced ensemble). Left panels: summer (DJF) and right panels: winter (JJA). Upper panels: RCP4.5; Lower panels: RCP8.5

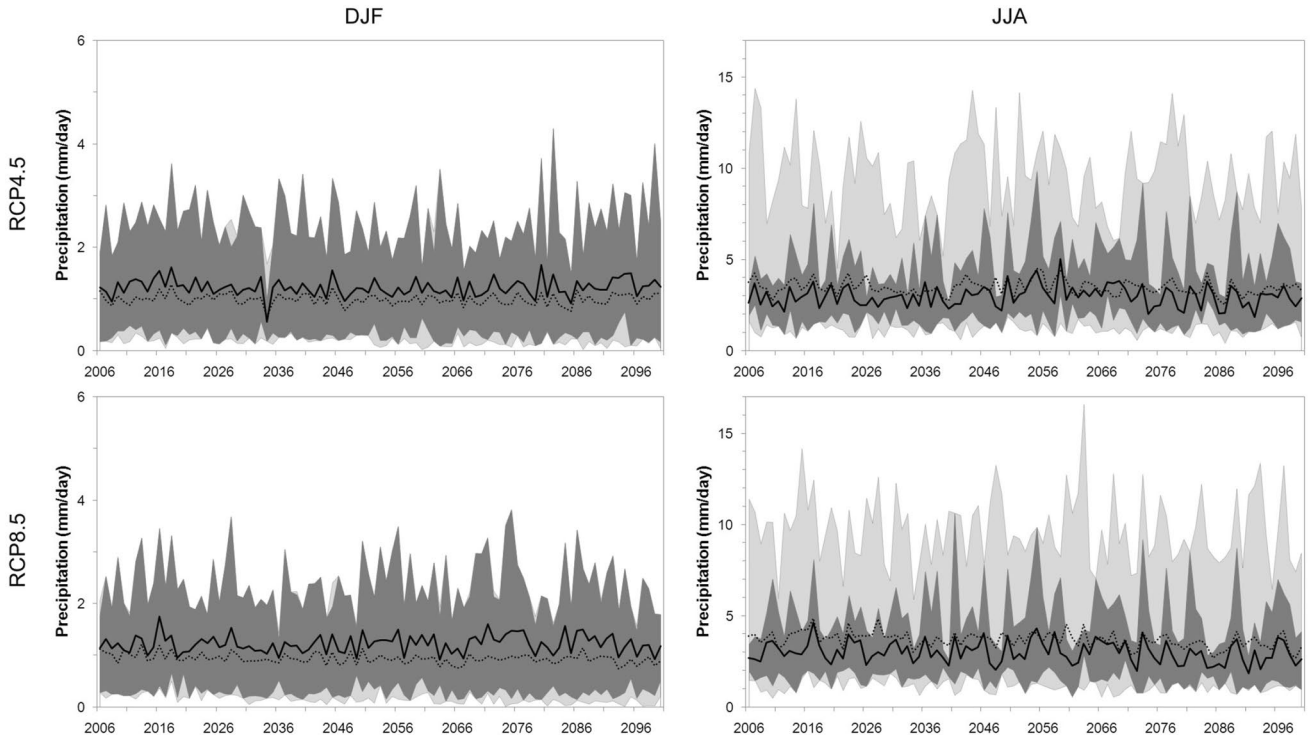

Fig. 4 Same as Fig. 3 but for precipitation

significant negative values: CCSM4 and EC-EARTH. These GCMs have shown a good agreement in the spatial distribution and the annual cycle of precipitation with the reference datasets in the period 1980–2005 (Zazulie et al. 2017). However, while EC-EARTH coincided with the negative trends shown in the reference datasets, CCSM4 showed the opposite behavior.

Changes in the spatial distribution of summer and winter temperature, relative to 1980–2005, for the reduced ensemble MMM5, are shown in Fig. 5, following RCP4.5 and RCP8.5 for two periods in the future: 2040–2065 and 2075–2100. All differences are positive, consistent with warming over the entire region. Note that larger changes are expected over high altitude areas compared to lowlands for both scenarios and future time frames. Projected differences are larger in the northern sector of the southern central Andes, where higher elevations are found. As expected, for both seasons the results for RCP8.5 show greater warming than for RCP4.5 and both scenarios present larger differences by the end of the twenty-first century.

Figure 6 shows projected changes in summer and winter precipitation relative to 1980–2005, for RCP4.5 and RCP8.5. The same spatial pattern of differences in summer precipitation is shown for both scenarios and for the two periods in the future: 2040–2065 and 2075–2100. All cases show a projected increase in summer precipitation east of the Andes, in the northern sector of the four left panels. The projected increase from 1980 to 2005 to 2040–2065 is about 4 mm/day, which represents an increase of 40% compared to the MMM5 climatology. In contrast, the reduced ensemble projects a decrease over central Chile. Projected winter precipitation differences are also shown in Fig. 5; note that the color scale is adjusted to the climatological values of precipitation in this season in order to better emphasize changes. For the period 2040–2065, MMM5 shows no change in the precipitation pattern for RCP4.5, while RCP8.5 indicates a slight decrease in winter precipitation over central Chile (centered at about 35°S). Both scenarios indicate negative differences in this same region by the end of the twenty-first century. The largest decrease (− 1 mm/day) is expected over Chile at around 35°S, where mean winter precipitation is close to 5 mm/day, representing a 20% decrease.

As was shown in Fig. 5, greater warming is expected around the border between Argentina and Chile where higher elevations in the Andes are found. To further explore this feature we present in Fig. 7 the temperature change as a function of elevation for the Subtropical Central Andes box for the five individual GCMs included in the reduced ensemble. While all projections show increases as a function of elevation there are some noteworthy seasonal differences. In summer (top panels in Fig. 7), models following RCP4.5 project a 1–2 °C increase for mid-century and a 2–3 °C increase by the end of the century. An increased warming is expected when following RCP8.5 and results in larger

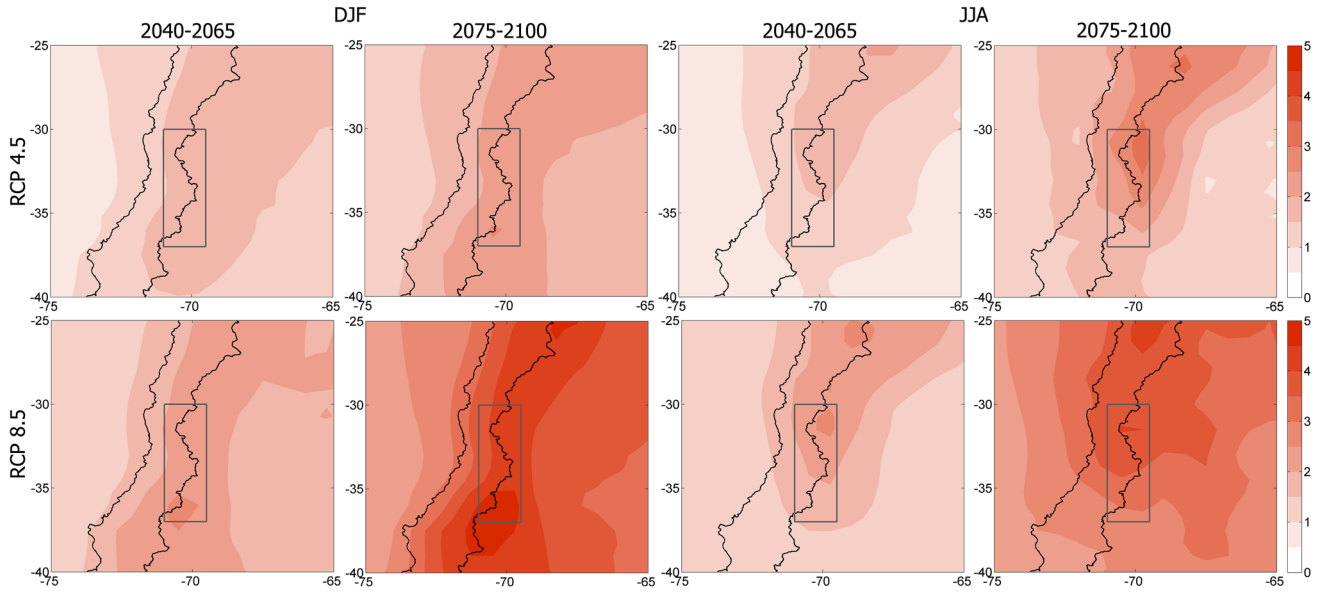

Fig. 5 Temperature changes (°C) relative to 1980–2005, obtained from the reduced ensemble (MMM5) for RCP4.5 (top) and RCP8.5 (bottom), for the periods 2040–2065 and 2075–2100. Left panels correspond to austral summer (DJF) and right panels to austral winter (JJA). The SCA box is delimited by the grey rectangle

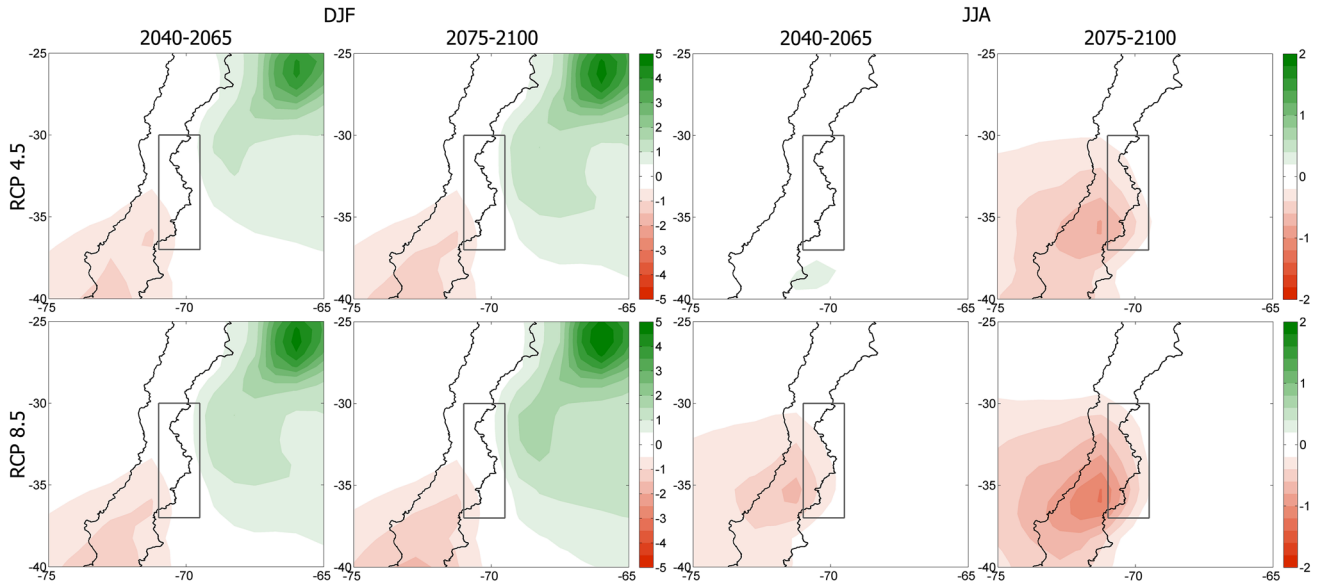

Fig. 6 Same as Fig. 5 but for precipitation. Note that the color scale is adjusted to the seasonal values

differences with respect to 1980–2005: about 2 °C by mid-century and 3–5 °C by late twenty-first century. There is a slight, but noticeable, dependence of the temperature change with elevation during summer. This relationship is further enhanced in winter, especially for RCP8.5, and also a greater temperature difference is observed between the two time frames. It is important to point out that each individual GCM presents an elevation dependence warming with slightly different slopes, which are related to the different representation of the topography in each model. The significance of these slopes was assessed with a Student's t-test, with the level of significance taken as $P < 0.05$. In winter, All 5 GCMs presented a positive significant linear relationship for both scenarios and both time frames. In contrast, in summer slopes resulted smaller than in winter and generally positive, except for RCP4.5 for the period 2075–2100 in CNRM-CM5 and EC-EARTH models. All slopes resulted significant under RCP4.5 for mid-century, while only CESM1-CAM5 resulted

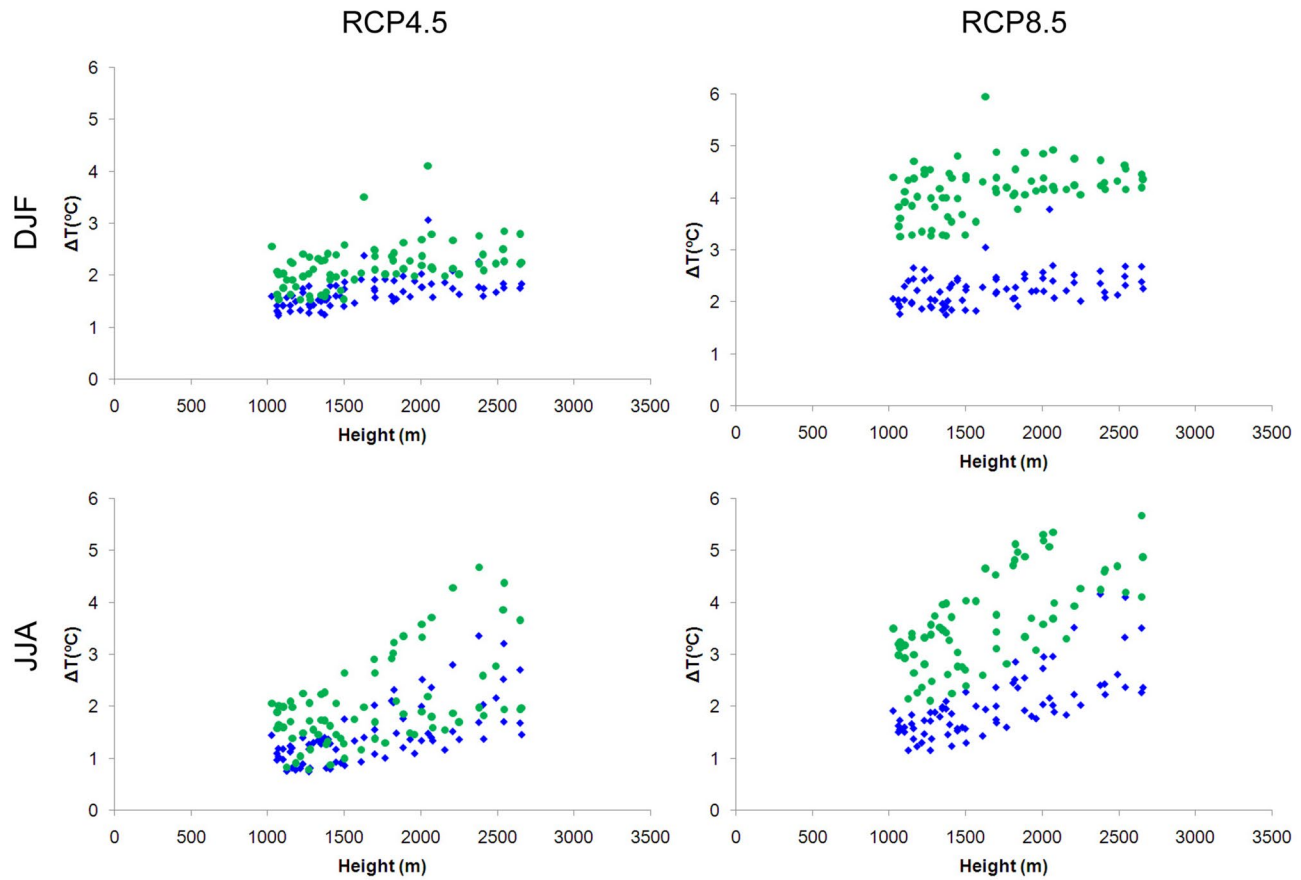

Fig. 7 Temperature change (°C) relative to 1980–2005, as a function of elevation for RCP 4.5 (left column) and RCP 8.5 (right column). Blue symbols correspond to 2045–2065 and green symbols to 2075–2100. Upper panels: austral summer (DJF); lower panels: austral winter (JJA)

significant under RCP8.5. For the end of the century, only CCSM4 and CESM1-CAM5 resulted significant under both scenarios.

This enhanced warming with elevation has been discussed in previous studies for other regions of the world (e.g. Bradley et al. 2004; Rangwala et al. 2013), and a possible mechanism relates to changes in the radiation budget as a result of changes in surface albedo. The SCA region is characterized by the presence of seasonal snowpack and permanent mountain glaciers. Changes in the spatial distribution of snow and ice at the surface will induce changes in albedo. Figure 7 shows the changes in summer and winter albedo as a function of elevation, for the two time frames using RCP8.5. Firstly, note that there are no changes projected in summer albedo (Fig. 8, left panel) for neither mid- nor late twenty-first century, relative to 1980–2005. The results for winter also show no changes at elevations lower than 1500 m, but there is an evident, non-linear decrease in albedo at higher elevations. The majority of the GCMs show albedo decreases between 20–60% at elevations higher than 1500 m. The exception is BCC-CSM1(m) that shows very small decreases in albedo, smaller than 1%. Differences for the ensemble mean at high altitude regions present a reduction of 22% percent for the period 2040–2065, and 32% by the end of the twenty-first century. The SCA region is characterized by a south-north gradient in elevation and an opposite gradient in annual precipitation, so that the maxima in snow cover and mountain glaciers are expected at approximately 35°S. It is likely that the morphology of the region combined with the atmospheric circulation (and resulting precipitation) may explain the non-linear relationship between changes in albedo and elevation.

A similar analysis is presented for precipitation (Fig. 9) in order to explore whether this variable shows an elevation-dependence. As seen in Fig. 9, the results are more variable than the clear signal observed for the temperature changes (Fig. 7). During austral summer, and at elevations lower than 2000 m, the majority of the points indicate either no change or a decrease in precipitation, while a majority of points indicate a precipitation increase at higher elevations. During austral winter the majority of the points indicate either no change or a decrease in precipitation, with little evidence of a relationship with elevation. Since there is little or no dependence on elevation of the change in precipitation,

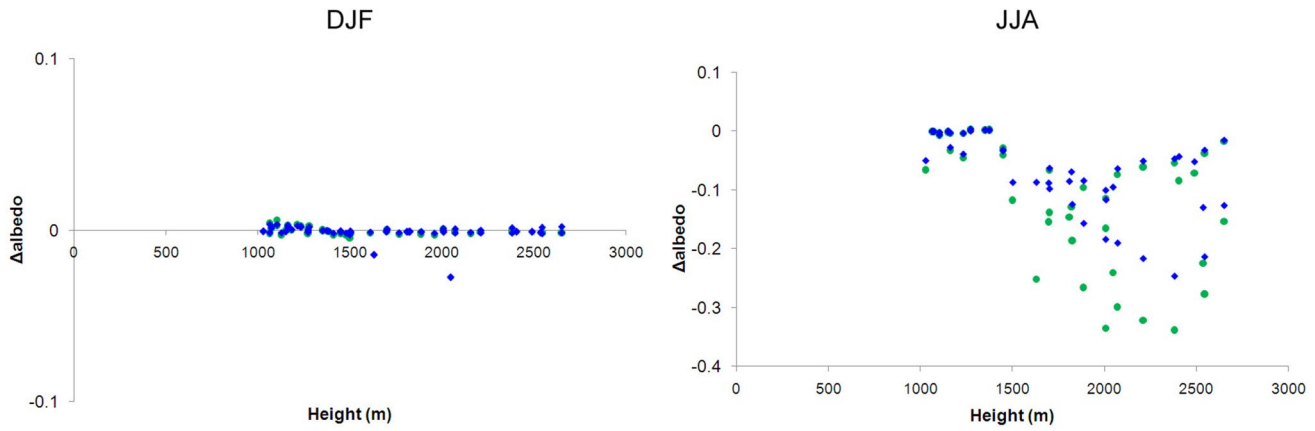

Fig. 8 Albedo change (relative to 1980–2005) as a function of elevation for summer (left column) and winter (right column), following RCP8.5. Blue symbols correspond to 2045–2065 and green dots to 2075–2100

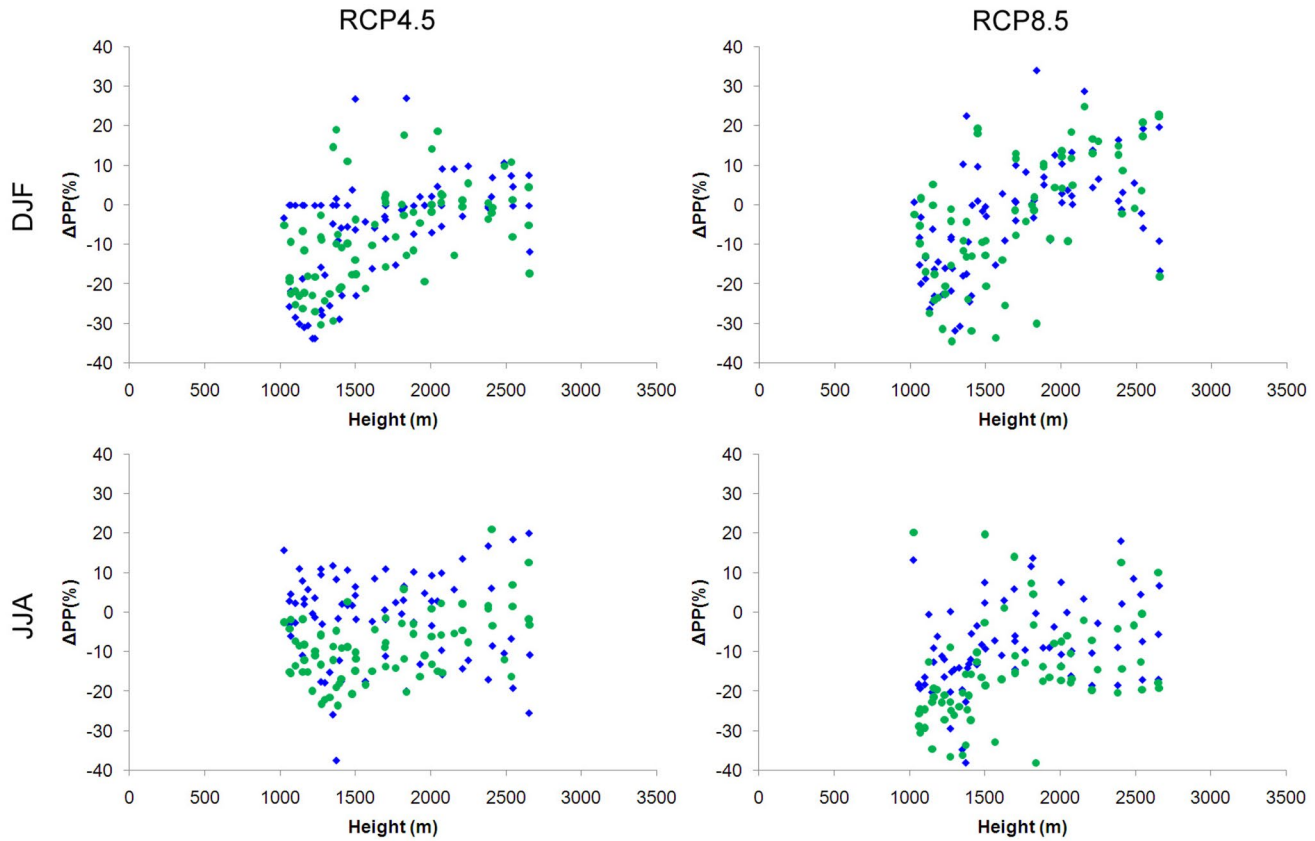

Fig. 9 Same as Fig. 7 but for precipitation change (%)

projected differences in circulation might be more useful in explaining changes in this variable.

Figure 10 shows the changes in 850 hPa humidity and wind, and sea level pressure for summer and winter from the MMM5 following RCP8.5 for the late twenty-first century. Only this scenario and time frame are shown because changes in summer precipitation are consistent across scenarios and time frames and larger changes are expected in winter with RCP8.5 for the period 2075–2100. As discussed in Z17, the summer low-level jet is responsible for precipitation in northern and northwest Argentina, east of the Andes. The MMM5 projects an increase in summer precipitation

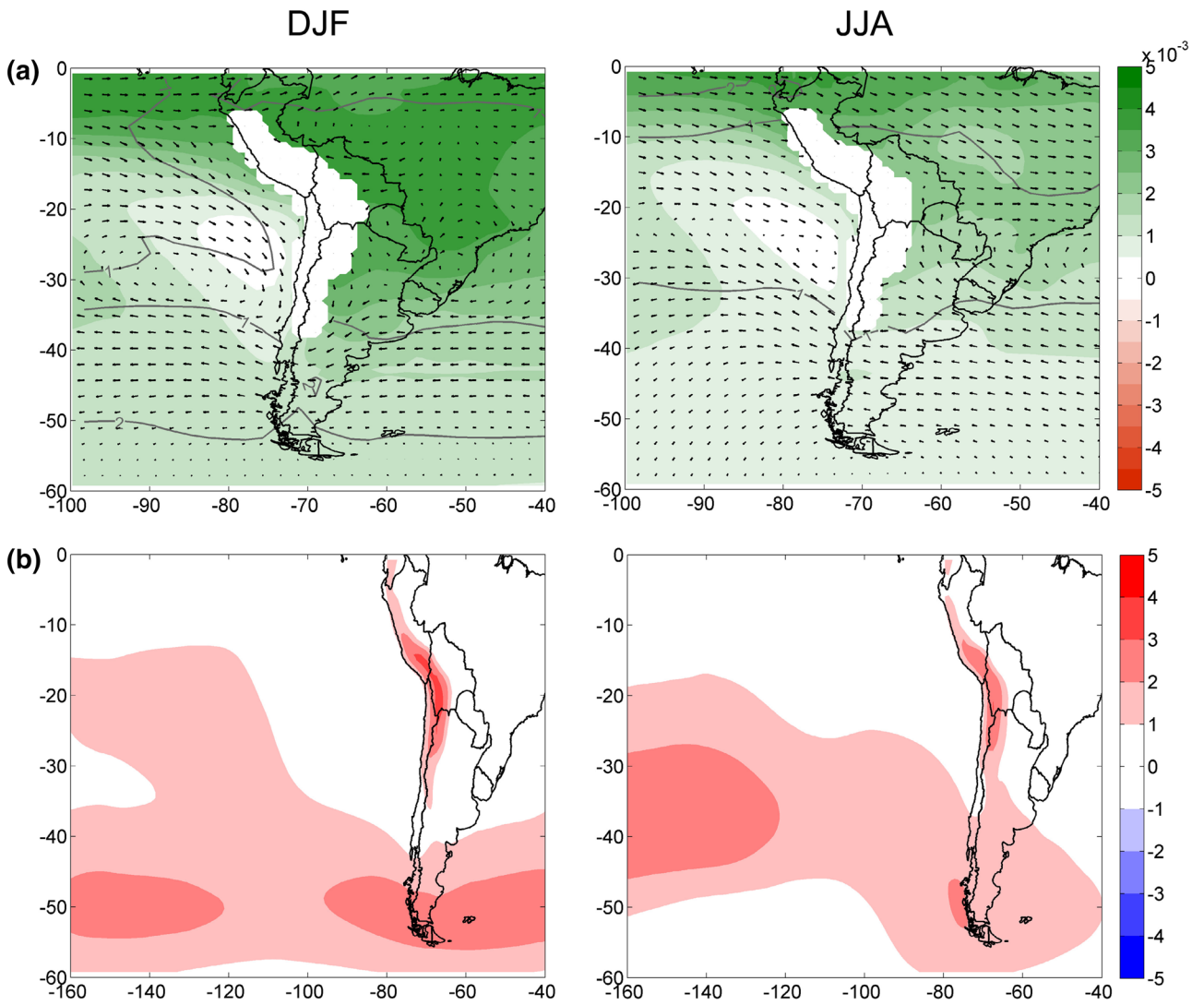

Fig. 10 Differences in **a** humidity (shaded) and wind (direction as vectors and intensity in contours) and **b** sea level pressure (hPa) between 2075 and 2100 using RCP8.5 and the historical run for the period 1980–2005 for summer (left) and winter (right)

east of the Andes (see Fig. 6). As seen in Fig. 10, there is an increase in low-level humidity in summer and a southerly wind anomaly, resulting in increased moisture advection into the region. West of the Andes a decrease in summer precipitation is projected from RCP8.5 simulations over central Chile, possibly associated with positive anomalies in surface pressure combined with a stronger anticyclonic circulation. The location of the south Pacific subtropical high modulates the annual cycle of precipitation over central Chile, influencing winter precipitation over the Andes. The MMM5 simulations following RCP8.5 project decreased winter precipitation by the late twenty-first century. Stronger positive pressure differences in sea level pressure in winter may indicate a displacement of the subtropical high farther away from the continent and combined with slightly reduced westerlies and stronger anticyclonic flow between 30° and 40°S, would result in less moisture advection during winter over the Subtropical Central Andes.

4 Summary and conclusions

Over 10 million people live in central Chile and central-western Argentina, adjacent to the Subtropical Central Andes. The population depends on fresh water originating from seasonal snowpack melting for human consumption, industry, irrigation and hydro-electric generation. In this study we provide detailed information of future climate projections for the region, crucial for determining future environmental policies of cryosphere conservation and water management in the region.

A common practice to assess future climate projections is to use the mean values of all climate models available. Historical simulations of fifteen GCMs were available at relatively high resolution and were analyzed in our previous study, Z17. The multi-model ensemble mean was obtained from those models (MMM15) and validated against ERA-Interim and the gridded CRU as reference datasets. The evaluation of model performance for the past climate (1980–2005) described in Z17, showed different abilities of individual GCMs in representing the climate of the SCA, suggesting that a reduced ensemble of only five members (MMM5) would better represent the regional climate. In the present study we have compared temporal series of temperature and precipitation for austral summer and winter between the full MMM15 and the reduced MMM5 over the SCA. It is evident that the MMM5 outperforms the MMM15 for both variables and both seasons. Whereas in summer there is a very small reduction in the bias for temperature and precipitation, in winter there is a large improvement in performance when using MMM5 compared against the two reference datasets. This improved performance justifies the selection of the reduced ensemble to evaluate climate projections for this region characterized by complex topography.

Future projections indicate warming during the twenty-first century over the SCA region, especially pronounced over the mountains. During winter, increases in temperature relative to 1980–2005 of up to 2.5 °C by 2040–2065 are simulated. A warming of up to 5 °C is projected for the highest elevations by the end of the century. This evidence of an elevation-dependence warming over the central Andes has also been reported in other mountain ranges around the world, e.g. in the Rockies and the Himalayas (Rangwala et al. 2013; Palazzi et al. 2016). Such a large monthly-mean warming during winter would most likely result in late winter-early spring snowpack melting, with serious implication for water availability during summer, when precipitation is negligible over the mountains. Moreover, linear trends for the period 2006–2100 indicate significant positive values for each of the GCMs analyzed and for the MMM5. Similar temperature trends are obtained for summer and winter but their magnitudes depend on the scenarios, approximately 0.2 °C/decade for RCP4.5 and close to 0.5°/decade using RCP8.5. The trend determined from the high emission scenario is twice the value of the trend obtained from the stabilization scenario.

A strong dependence of the temperature trends on elevation was found in winter for both time frames, and it is enhanced for the RCP8.5 scenario. This relationship is weaker in summer. Our results are consistent with previous studies that explored EDW over other mountain ranges in the world. The EDW has been related to changes in the net flux of energy at the surface as a result of changes in surface albedo. In the Himalayas, Palazzi et al. (2016) found that surface albedo was the dominant factor to the observed EDW. Nevertheless, other factors such as elevation-dependent changes in cloud cover and soil moisture have also been suggested as possible forcings (Pepin et al. 2015) and could prevail at some other elevated regions. The SCA is characterized by the presence of seasonal snowpack and mountain glaciers that are directly affected by EDW, which in turn induces changes in the surface albedo. A strong reduction in albedo (between 20–60%) for elevated sites in winter is evident from the simulations, while no albedo change is found in summer. The relationship in winter is non-linear and may be explained by the morphology of the region combined with the atmospheric circulation.

No clear trend was identified for precipitation in the SCA region. Spatial patterns of changes in this variable showed a consistent increase in summer precipitation across scenarios and time frames in northwestern Argentina. This region was identified in our previous study (Z17) as due to the mis-representation of summer mechanisms involved in the generation of convective precipitation from GCMs and reanalysis, so results in this region are considered less reliable. A decrease in winter precipitation in central Chile was found for RCP4.5 only for the end of the twenty-first century, and for RCP8.5 for both time frames.

The combined projections of increased temperature, reduced albedo and reduced precipitation in winter could lead to severe restrictions in the water availability in the region of the Subtropical Central Andes and large societal consequences on both sides of the Andes.

Acknowledgements We thank the anonymous reviewers for their valuable comments. This work has been supported by project UBA-501 20020130200142BA from the University of Buenos Aires. We acknowledge the Program for Climate Model Diagnosis and Intercomparison (PCMDI) for collecting and archiving the CMIP5 model output. We are grateful to the ECWMF and the CRU for providing reanalysis and gridded observed data sets. Finally, we thank Dr. D. Baumgardner for the editorial and language review of the manuscript.

References

Aceituno P, Fuenzalida H, Rosenbluth B (1993) Climate along the extratropical west coast of South America. In: Mooney HA, Fuentes ER, Kronberg BI (eds) Earth system responses to global change: contrasts between North and South America. Academic Press, New York, pp 61–72

Barros V, Castañeda ME, Doyle M (2000) Recent precipitation trends in southern South America east of the Andes: An indication of climate variability. In: Smolka PP, Volkheimer W (eds) Southern Hemisphere Paleo and Neo-Climates. Springer, Berlin, pp 187–206

Barros VR, Boninsegna JA, Camilloni IA, Chidiak M, Magrín GO, Rusticucci M (2015) Climate change in Argentina: trends, projections, impacts and adaptation. WIREs Clim Change. https://doi.org/10.1002/wcc.316

Beniston M (2003) Climatic change in mountain regions: a review of possible impacts. Clim Change 59:5–31. https://doi.org/10.1023/A:1024458411589

Beniston M, Diaz H, Bradley R (1997) Climatic change at high elevation sites: an overview. Clim Change 36:233–251

Blazquez J, Nuñez MN (2013) Analysis of uncertainties in future climate projections for South America: comparison of WCRP-CMIP3 and WCRP-CMIP5 models. Clim Dyn 41:1039–1056. https://doi.org/10.1007/s00382-012-1489-7

Bradley RS, Keimig FT, Diaz HF (2004) Projected temperature changes along the American cordillera and the planned GCOS network. Geophys Res Lett 31:L16210. https://doi.org/10.1029/2004GL020229

Bradley RS, Vuille M, Diaz HF, Vergara W (2006) Threats to water supplies in the tropical Andes. Science 312:1755–1756

Falvey M, Garreaud RD (2009) Regional cooling in a warming world: recent temperature trends in the southeast Pacific and along the west coast of subtropical South America (1979–2006). J Geophys Res 114:D04102. https://doi.org/10.1029/2008JD010519

Fyfe JC, Flato GM (1999) Enhanced climate change and its detection over the Rocky Mountains. J Clim 12:230–243

Le Quesne C, Acuña C, Boninsegna J, Rivera A, Barichivich J (2009) Long-term glacier variations in the Central Andes of Argentina and Chile, inferred from historical records and tree-ring reconstructed precipitation. Palaeoecology 281:234–244

Liu X, Cheng Z, Yan L, Yin Z-Y (2009) Elevation dependency of recent and future minimum surface air temperature trends in the Tibetan Plateau and its surroundings. Glob Planet Change 68:164–174. https://doi.org/10.1016/j.gloplacha.2009.03.017

Masiokas MH, Villalba R, Luckman B, Le Quesne C, Aravena JC (2006) Snowpack variations in the central Andes of Argentina and Chile, 1951–2005: large-scale atmospheric influences and implications for water resources in the region. J Clim 19:6334–6352. https://doi.org/10.1175/JCLI3969.1

Minetti JL, Vargas WM (1998) Trends and jumps in the annual precipitation in South America south of the 15°S. Atmosfera 11:205–221

Minetti JL, Vargas WM, Poblete AG, Acuña LR, Casagrande G (2003) Non-linear trends and low frequency oscillations in annual precipitation over Argentina and Chile, 1931–1999. Atmosfera 16:119–135

Moss RH, Edmonds JA, Hibbard KA, Manning MR, Rose SK, van Vuuren DP, Carter TR, Emori S, Kainuma M, Kram T, Meehl GA, Mitchell JFB, Nakicenovic N, Riahi K, Smith S, Stouffer RJ, Thomson AM, Weyant JP, Wilbanks TJ (2010) The next generation of scenarios for climate change research and assessment. Nature 463:747–756. https://doi.org/10.1038/nature08823

Palazzi E, Filippi L, von Hardenberg J (2016) Insights into elevation-dependent warming in the Tibetan Plateau-Himalayas from CMIP5 model simulations. Clim Dyn. https://doi.org/10.1007/s00382-016-3316-z

Palomino-Lemus R, Córdoba-Machado S, Gámiz-Fortis SR, Castro-Díez Y, Esteban-Parra MJ (2015) Summer precipitation projections over northwestern South America from CMIP5 models. Global Planet Change 131:11–23

Pepin N, Bradley RS, Diaz HF, Baraer M, Caceres EB, Forsythe N, Fowler H, Greenwood G, Hashmi MZ, Liu XD, Miller JR, Ning L, Ohmura A, Palazzi E, Rangwala I, Schöner W, Severskiy I, Shahgedanova M, Wang MB, Williamson SN, Yang DQ (2015) Elevation dependent warming in the mountain regions of the world. Nat Clim Change 5:424–430. https://doi.org/10.1038/NCLIMATE2563

Rangecroft S, Suggitt AJ, Anderson K, Harrison S (2016) Future climate warming and changes to mountain permafrost in the Bolivian Andes. Clim Change 137:231–243. https://doi.org/10.1007/s10584-016-1655-8

Rangwala I, Sinsky E, Miller JR (2013) Amplified warming projections for high altitude regions of the northern hemisphere midlatitudes from CMIP5 models. Environ Res Lett 8:024040

Rangwala I, Sinsky E, Miller JR (2016) Variability in projected elevation dependent warming in boreal midlatitude winter in CMIP5 climate models and its potential drivers. Clim Dyn 46:2115–2122. https://doi.org/10.1007/s00382-015-2692-0

Riahi K, Rao S, Krey V, Cho C, Chirkov V, Fischer G, Kindermann G, Nakicenovic N, Rafaj P (2011) RCP 8.5-a scenario of comparatively high greenhouse gas emissions. Clim Change 109:33–57. https://doi.org/10.1007/s10584-011-0149-y

Rosenblüth B, Fuenzalida H, Aceituno P (1997) Recent temperature variations in southern South America. Int J Climatol 17:67–85

Rusticucci M, Zazulie N, Raga GB (2014) Regional winter climate of the southern central Andes: assessing the performance of ERA-Interim for climate studies. J Geophys Res 119:8568–8582. https://doi.org/10.1002/2013JD021167

Stocker TF, Qin D, Plattner G-K, Alexander LV, Allen SK, Bindoff NL, Bréon F-M, Church JA, Cubasch U, Emori S, Forster P, Friedlingstein P, Gillett N, Gregory JM, Hartmann DL, Jansen E, Kirtman B, Knutti R, Kumar KK, Lemke P, Marotzke J, Masson-Delmotte V, Meehl GA, Mokhov II, Piao S, Ramaswamy V, Randall D, Rhein M, Rojas M, Sabine C, Shindell D, Talley LD, Vaughan DG, Xie S-P (2013) Technical summary. In: Stocker TF, Qin D, Plattner G-K, Tignor M, Allen SK, Boschung J, Nauels A, Xia Y, Bex V, Midgley PM (eds) Climate Change 2013: The Physical Science Basis. Contribution of Working Group I to the Fifth Assessment Report of the Intergovernmental Panel on Climate Change. Cambridge University Press, Cambridge

Taylor KE, Stouffer RJ, Meehl GA (2012) An over-view of CMIP5 and the experiment design. Bull Am Meteorol Soc 93:485–498. https://doi.org/10.1175/BAMS-D-11-00094.1

Thomson AM, Calvin KV, Smith SJ, Kyle GP, Volke A, Patel P, Delgado-Arias S, Bond-Lamberty B, Wise MA, Clarke LE, Edmonds JA (2011) RCP4.5: a pathway for stabilization of radiative forcing by 2100. Clim Change 109:77–94, https://doi.org/10.1007/s10584-011-0151-4

van Vuuren DP, Edmonds J, Kainuma M, Riahi K, Thomson A, Hibbard K, Hurtt GC, Kram T, Krey V, Lamarque J-F, Masui T, Meinshausen M, Nakicenovic N, Smith SJ, Rose SK (2011) The representative concentration pathways: An overview. Clim Change 109:5–31. https://doi.org/10.1007/s10584-011-0148-z

Viale M, Nuñez MN (2011) Climatology of winter orographic precipitation over the subtropical central Andes and associated synoptic and regional characteristics. J Hydrometeorol 12:481–507. https://doi.org/10.1175/2010JHM1284.1

Vincent LA, Peterson TC, Barros VR, Marino MB, Rusticucci M, Carrasco G, Ramirez E, Alves LM, Ambrizzi T, Berlato MA, Grimm AM, Marengo JA, Molion L, Moncunill DF, Rebello E, Anunciação YMT, Quintana J, Santos JL, Baez J, Coronel G, Garcia J, Trebejo I, Bidegain M, Haylock MR, Karoly D (2005) Observed trends in indices of daily temperature extremes in South America 1960–2000. J Clim 18:5011–5023. https://doi.org/10.1175/JCLI3589.1

Viviroli D, Dürr HH, Messerli B, Meybeck M, Weingartner R (2007) Mountains of the world, water towers for humanity: typology, mapping, and global significance. Water Resour Res 43:W07447. https://doi.org/10.1029/2006WR005653

Vuille M, Francou B, Wagnon P, Juen I, Kaser G, Mark BG, Bradley RS (2008) Climate change and tropical Andean glaciers: past, present and future. Earth Sci Rev 89:79–96. https://doi.org/10.1016/j.earscirev.2008.04.002

Zazulie N, Rusticucci M, Raga GB (2017) Regional climate of the subtropical central Andes using high-resolution CMIP5 models. Part I: past performance (1980–2005). Clim Dyn 49:3937. https://doi.org/10.1007/s00382-017-3560-x

Zubler EM, Fischer AM, Fröb F, Liniger MA (2015) Climate change signals of CMIP5 general circulation models over the Alps—impact of model selection. Int J Climatol. https://doi.org/10.1002/joc.4538